Reconfigurable Bandpass Filter With a Three-to-One Switchable Passband Width

Christen Rauscher, *Fellow, IEEE*

***Abstract*—A reconfigurable bandpass filter is described that aims to preserve the optimal performance of a broad-band system under changing signal conditions. It does so by allowing the passband width of the system's receiver to adapt. The filter can be switched between two discrete states with widely differing bandwidths of 500 and 1500 MHz, respectively, while keeping the passband responses centered at 10 GHz. The physical implementation comprises a hybrid-integrated microstrip circuit on a 0.010-in-thick quartz substrate. The circuit employs commercial beam-lead p-i-n diodes to switch fixed-valued reactance elements. Despite the presence of semiconductor switching devices, the filter behaves very linearly, exhibiting measured passband third-order output-referenced intercept points that exceed 46 dBm in both switched states.**

***Index Terms*—Bandpass, discrete tuned, microwave filter, miniature, reconfigurable, switched, tunable.**

I. Introduction

A TREND IN modern high-frequency system design is to employ broad receiver bandwidths that can simultaneously support multiple information channels. This places stringent demands on receiver front-end electronics, particularly with regard to dynamic range. A preselection filter can be an important instrument in the preservation of dynamic range. The filter may be assigned a bandpass response for retaining signal content within a predetermined frequency band of interest, while suppressing noise contributions and interference from outside the band. Alternatively, the preselection function may be carried out by a band-reject filter to exclude unwanted spectral components interfused with wanted signals. Due to the often fluent nature of signal conditions in the field, the preselection circuit may need to be adaptive. This can be achieved with either a bank of switchable fixed-frequency filters or a single filter with variable frequency characteristics.

In recent years, efforts have been devoted to deriving new compact tunable microwave filters that offer size advantages over alternative filter-bank solutions. Frequency tuning is normally accomplished with reactance elements whose reactance values can either be varied in a continuous fashion or be changed by discrete amounts. Continuous tuning has had the widest following, with prominent reliance on semiconductor varactors and magnetically tuned YIG resonators as variable reactance elements [1]. Tuning of filter characteristics in discrete frequency steps has been gaining in popularity though, with the introduction of microelectromechanical switching devices. Such are employed as alternatives to conventional p-i-n diodes, in conjunction with sets of switchable fixed-reactance elements [2], [3]. In situations where fine-scale tuning over a narrow-to-moderate frequency span is required, varactor-tuned filters generally involve the least amount of circuit complexity. This is achieved often at the cost of relatively high varactor-related dissipation losses and signal-distortion levels. Discrete-tuned filters are especially attractive for covering broad tuning ranges. However, circuit complexity and the potential for deleterious parasitic effects can become a concern, when a large number of tuning steps are involved that require a commensurate number of switchable reactance elements and associated bias circuits. Tuning-element-derived dissipation losses and signal distortion in such filters tend to not figure among critical performance constraints. They are more likely to be dominated by conductor losses, especially in planar-circuit filters, and by the presence of active semiconductor components elsewhere in the receiver front-end circuitry.

In the past, work on tunable high-frequency filters [1] has concentrated largely on varying passband center frequencies of bandpass filters and stopband center frequencies of band-reject and notch filters. For the most part, bandwidth tuning has been deliberately kept within modest bounds or avoided altogether. The work reported here, in contrast, focuses entirely on achieving broad-ranged variability of a filter's passband width. To minimize signal distortion, the bandpass filter chosen for demonstration relies on a passive-circuit architecture, combined with discrete tuning. The circuit is believed to represent the first reconfigurable or discrete-tuned bandpass filter to be reported with a three-to-one variability of its passband width around an invariant passband center frequency.

II. Filter Design

When compared to a bandpass filter with a variable center frequency, the design of a filter with a variable passband width can present a more formidable challenge. This is especially true for a passband width that is to be tuned over a very wide range, as is assumed here. Center-frequency tuning primarily involves the shifting of natural frequencies of individual filter resonators, whereby the general shape of a filter's frequency response is largely maintained. Conversely, altering a filter's relative bandwidth, by its very nature, modifies the intrinsic shape of the response curve, realized with the help of commensurate changes in the coupling among filter resonators. To maintain optimal

Manuscript received June 25, 2002; revised August 21, 2002.

The author is with Code 6850.1, Naval Research Laboratory, Washington, DC 20375-5347 (e-mail: rauscher@ieee.org).

Digital Object Identifier 10.1109/TMTT.2002.807818

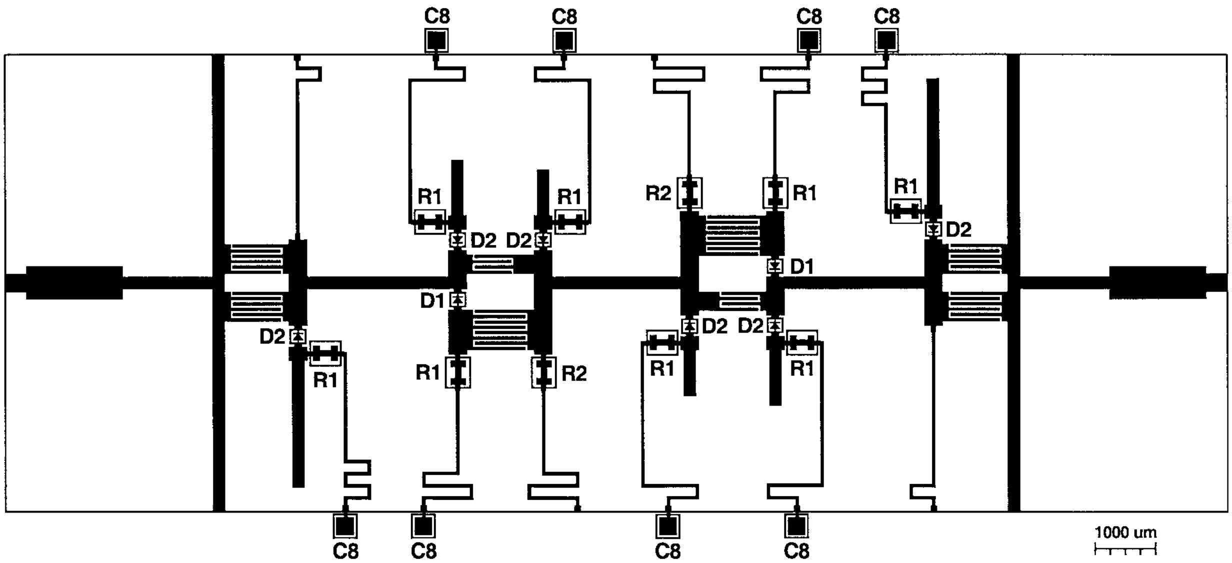

Fig. 1. Circuit layout of the reconfigurable variable-bandwidth bandpass filter.

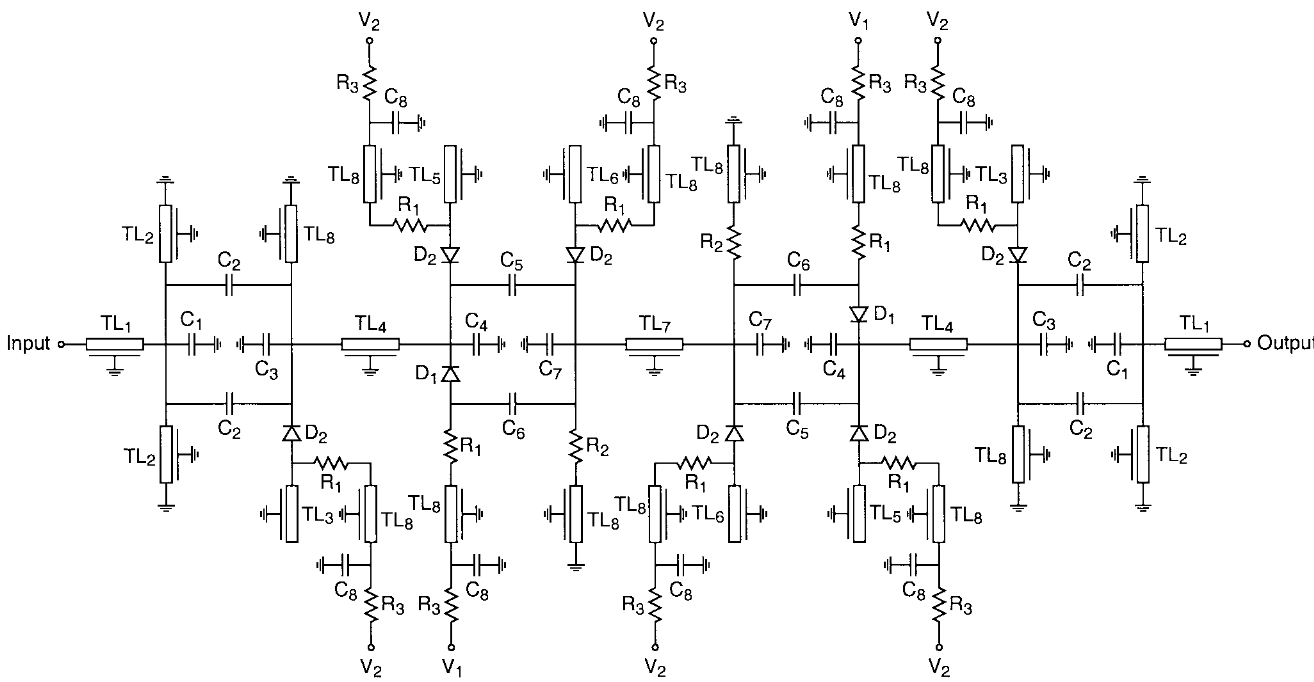

Fig. 2. Equivalent-circuit of the reconfigurable bandpass filter.

characteristics over a broad designated bandwidth tuning range, each reactive filter element should ideally be allowed to vary in an independent fashion. The challenge is to find a circuit architecture that provides adequate variability without requiring an excessive number of tuning elements, and without producing deleterious response anomalies at extreme settings.

In a reconfigurable filter, the order of its response characteristics could readily be varied within the context of the reconfiguration process. For narrow-band signals, it may be useful to increase the effective order of the filter in its narrowest band settings to enhance selectivity. It may be equally helpful, in other situations, to decrease the filter's effective order, and thereby accept less flank steepness in return for reduced passband attenuation. Leaving the filter order essentially unchanged, as in the current case, can provide a reasonable compromise between filtering attributes and circuit complexity.

The present reconfigurable bandpass filter example is empirically derived. The microstrip design employs a mix of quasi-lumped and distributed circuit elements, with p-i-n diodes used for reactance-switching purposes. The physical layout of the microstrip conductor pattern is shown in Fig. 1, realized on a 0.010-in-thick quartz substrate. Also included, for the sake of reference, are the outlines of discrete circuit components added to the microstrip structure. Aside from the p-i-n diodes already mentioned, the added components comprise a number of chip resistors and capacitors identified by pertinent labels. An equivalent-circuit diagram is provided in Fig. 2. The schematic is drawn to be point symmetric around the circuit's center in accordance with the actual physical layout. The filter is of the capacitive-end-coupled-resonator type, nominally comprised of four interdigital capacitive coupling structures connected in cascade with inductive segments of uniform transmission line. The coupling structures are represented by the clusters of lumped capacitors C_1 through C_3 and capacitors C_4 through C_7, whereby labels have been reused to denote circuit elements of the same value. As is evident in Fig. 1, the input and output coupling structures each consists of a pair of identical interdigital capacitors connected in parallel. Each of the other two coupling structures is likewise composed of two interdigital substructures that are connected also essentially in parallel, but with the substructures differing in size. The larger of the two can be switched in and out to vary the degree of inter-resonator coupling. All interdigital capacitors have a common finger width of 50 μm and a common finger separation of 37.5 μm. Capacitors associated with schematic elements C_2, C_5, and C_6 have six, three, and eight fingers, with finger lengths of 800, 600, and 825 μm, respectively. The cascade-connected resonator line segments TL_4 and TL_7 are of nominal 85-Ω characteristic impedance. They are realized as 200-μm-wide conductor strips, as are the impedance-transforming line segments at the circuit's input and output (TL_1) and the added short-circuited inductive transmission-line stubs (TL_2).

Switching between the filter's narrow-band and wide-band states is accomplished with p-i-n diodes D_1 and D_2, representing beam-lead devices of type MPN-1101–12 by MicroMetrics Inc., Londonderry, NH. To select the wide-band state, diodes D_1 are forward biased with 50 mA. This maximizes inter-resonator coupling through the parallel connection of respective interdigital capacitors identified by schematic elements C_5 and C_6. In this state, a reverse bias of -10 V is applied to diodes D_2 to isolate, from the main portion of the filter circuit, the capacitive shunt elements represented in the schematic by open-circuited transmission-line stubs TL_3, TL_5, and TL_6. To arrive at the filter's narrow-band state, the interdigital capacitors associated with schematic elements C_6 are disconnected at one of their respective terminals through reverse biasing of diodes D_1. In turn, the transmission-line stubs TL_3, TL_5, and TL_6 are connected to the circuit core by way of forward-biased diodes D_2. The combined influence is to reduce the coupling between filter resonators, and to also increase the effective lengths of the cascade-connected inductive transmission-line segments TL_4 and TL_7. The latter is required to prevent resonant frequencies from shifting upward with reduced inter-resonator coupling. Transmission-line elements TL_8 constitute quarter-wave-long segments of 135-Ω characteristic impedance, realized as 50-μm-wide microstrip traces. They provide bias to the p-i-n diodes, in conjunction with the 50-Ω series resistors R_1, the 25-Ω series resistors R_2, the 100-Ω series resistors R_3, and the 29-pF chip bypass capacitors C_8. The bias-circuit time constants defined by the resistor and capacitor values largely determine the speed with which the filter can be switched between states. With switching speed not an issue in the envisioned application, the filter's switching behavior did not figure among the design criteria. However, a rough estimate would indicate intrinsic switching times of less than 10 ns for the chosen implementation. Pertinent time constants could be reduced by decreasing the values of the discrete components. The series resistors R_1 and R_2, however, are needed to perform a useful damping function. They suppresses spurious responses that would otherwise occur as a result of maintaining essentially the same basic filter configuration and filter order in the presence of the sought-after very wide three-to-one bandwidth tuning ratio.

Counting only nonredundant circuit components, the filter comprises 17 principal reactance elements whose values should ideally all be permitted to vary when switching between reconfiguration states. Of these elements, seven are cascade connected, and the other ten are shunt connected to ground. Due to the distributed nature of the cascade-connected elements, including the quasi-lumped interdigital capacitors, two switches would normally be required to switch each of these elements in and out of the circuit. Only one switch is needed to accommodate each shunt-connected element. Thus, the total number of switches called for would be 24. In contrast, the present filter circuit utilizes only eight p-i-n-diode switches, one-third as many.

The reduced number of switches is made possible, in part, by identifying circuit elements whose optimum values for each of the two states differ only modestly, and then assigning fixed values to these elements. To make up for minor discrepancies in response characteristics that result from such approximations, numerical optimization techniques are used to adjust the remaining independent circuit parameters for the best compromise. To further minimize circuit complexity and overall size, dual functions are assigned to the various shunt-connected capacitance elements. Among these elements are ones that are native to the interdigital structures, with respective shunt-capacitance values selectively enhanced through the enlargement of pertinent contact regions. Other dual-function elements include the shunt-connected open-circuited transmission-line stubs that can be switched in and out with the help of p-i-n diodes D_2. When changing from the wide-band to the narrow-band state, the shunt-capacitance elements switched in with the help of the diodes add to the capacitive loading already provided by the fixed-valued shunt capacitors of the interdigital structures. One function of this is to reduce inter-resonator coupling through capacitive-voltage-divider action. The other function is to increase the effective electrical lengths of resonator transmission-line segments TL_4 and TL_7. As already mentioned, the latter is necessary to counteract the shifting of the resonators' natural frequencies due to the reduced coupling. Regarding the interdigital capacitors identified by the series-connected capacitors C_6, in particular, the shunt capacitance native to one terminal of each structure is fully absorbed into the capacitive-loading process as a fixed-valued contribution. This conveniently permits only one diode per structure instead of two diodes to be used for connecting and disconnecting pertinent elements, helping to achieve the mentioned three-to-one reduction in the number of switches required. As should be expected though, shortcuts like these invariably result in lost degrees of design freedom and

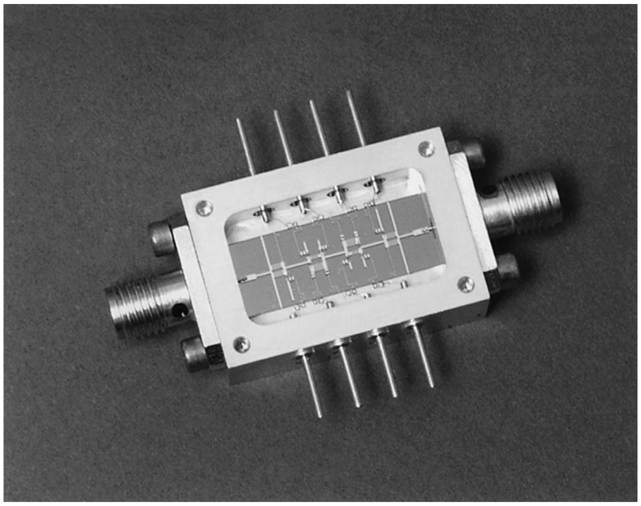

Fig. 3. Reconfigurable bandpass filter with passband centered at 10 GHz and bandwidth switchable between 500 and 1500 MHz, implemented in microstrip on a 0.010-in-thick quartz substrate.

in potential compromises with regard to filter characteristics. However, as the results described in the following demonstrate, accepted compromises are relatively minor and mainly involve the symmetry of the response curves.

III. Experimental Results

The reconfigurable bandpass filter in its hybrid-integrated form is depicted in Fig. 3. As mentioned earlier, the basic microstrip circuit pattern is realized on a 0.010-in-thick quartz substrate. The metallization thickness is 3 μm. Also already mentioned is the augmentation of the microstrip structure with sets of discrete components that include the beam-lead p-i-n diodes used for switching, and the various chip resistors and capacitors associated with the bias networks. All electrical connections between the microstrip circuit pattern and the discrete components are made with either conductive epoxy resin or with straps of gold ribbon. As should be apparent from the photograph, the circuit was designed more with ease of computation and implementation in mind than for smallest possible size, with the quartz substrate mounted inside the metal enclosure measuring 7.5 mm $\times$ 20 mm.

Measured filter responses for the wide-band and narrow-band settings are compared in Figs. 4 and 5 with their respective calculated counterparts. As the calculations do not include packaging effects, all measurements were subsequently performed with the cover removed, exactly as shown in the photograph. Very good agreement with regard to general frequency behavior is observed between corresponding measured and calculated curves. Only the passband attenuation values show some discrepancies, which are largely attributed to overoptimistic conductor-loss assumptions made by the commercial microwave design software used for the current task. Although the effects of the coaxial-to-microstrip launchers and those of parasitic coupling between interdigital structures were not included in the calculations, their combined contributions to passband insertion loss should account for only a few tenths of 1 dB. Other minor

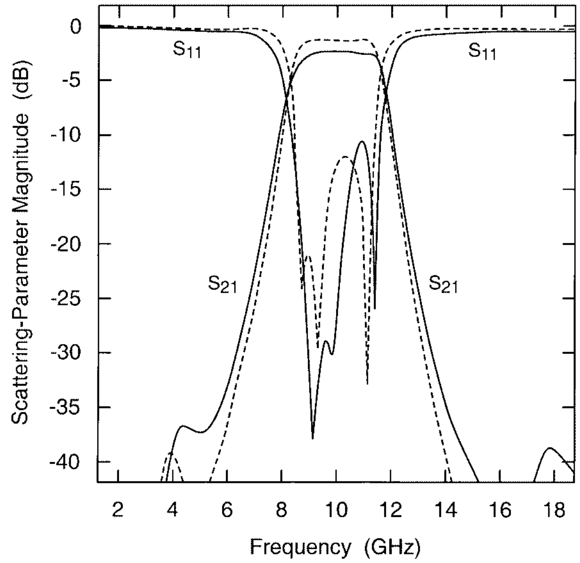

Fig. 4. Magnitude responses of filter transmission coefficient ($S21$) and reflection coefficient ($S11$) for the wide-passband setting: —— measured, – – calculated.

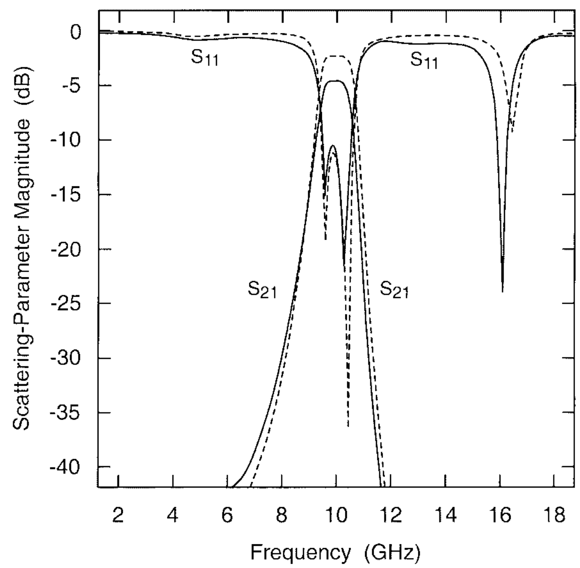

Fig. 5. Magnitude responses of filter transmission coefficient ($S21$) and reflection coefficient ($S11$) for the narrow-passband setting: —— measured, – – calculated.

discrepancies between corresponding curves are likely due to manufacturing tolerances.

When comparing the filter's calculated and measured responses for the wide-band setting with the corresponding curves for the narrow-band case, it may be noted that the respective decibel values for passband insertion loss differs roughly by a factor of two. For a change in bandwidth of three-to-one, as in the current situation, a commensurate ratio among insertion-loss numbers might be expected. In analyzing the apparent anomaly, it should be pointed out that radiation plays no role in this. Associated effects are neither included in the calculations, nor does the experimental circuit exhibit any sign of such. To confirm this, the circuit was temporarily

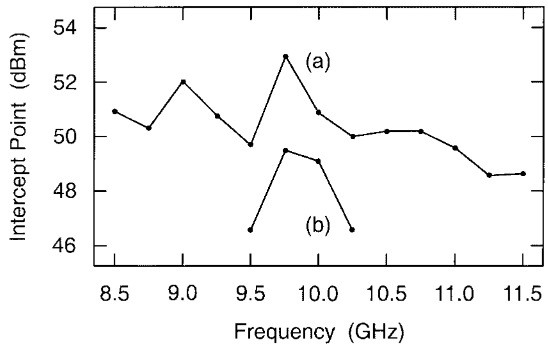

Fig. 6. Measured filter third-order-intercept output power levels. (a) Wide-passband setting. (b) Narrow-passband setting.

covered with the lid, showing no discernible change in passband insertion loss for both the wide-band and the narrow-band setting. Also unlikely, albeit possible culprits, are the parasitic series resistances of the switching diodes. With a conservative value of 2 Ω attributed to each diode resistance, calculations indicate that less than one-third of respective total insertion-loss values in each case, when measured in decibels, is due to the diodes. It is assumed that the same observation also applies to the experimental results. This leaves as the most likely cause of the passband-loss anomaly the topological differences, which are quite considerable, between the filter in its wide-band state and its narrow-band state.

To improve the filter's passband characteristics, strategically placed active circuit elements could have been integrated into the design. This would, however, have led to increased levels of signal distortion. In light of the envisioned system application, the use of active elements was not pursued. Nevertheless, even with the totally passive circuit configuration relied on here, the p-i-n-diode switches contribute some amount of signal distortion. To determine how much, intermodulation measurements were preformed on the filter in both of its states, using a two-tone method with tones separated in frequency by 1 MHz and stepped across respective passband intervals in 250-MHz increments. The measured values, after conversion to equivalent third-order output-referenced intercept points, are presented in Fig. 6. As expected, the narrow-band setting produces lower intercept-point values when compared to the wide-band setting. This is at least in part directly linked to passband attenuation. The observed waviness of the upper curve is likely the result of vector addition and subtraction among a multiplicity of signal distortion products within the filter, originating from the eight separate switching diodes. Overall, though, it should be noted that even the worst passband intercept-point value exceeds a very respectable level of 46 dBm.

IV. Summary and Conclusions

The reconfigurable bandpass filter described in this paper was inspired by a need to provide a receiver with the capability to change bandwidth in response to prevailing signal conditions. The circuit is a precursor to a filter that permits simultaneous tuning of both passband center frequency and bandwidth. Such is desired for broad-band applications that involve simultaneous independent signal transmissions. A discrete-tuned passive-circuit approach was chosen, relying on p-i-n-diode switching of fixed-valued reactance elements to minimize signal distortion and permit use of the filter in its designated preselection role. The challenge was to achieve a very large passband-width tuning ratio of three to one without compromising response characteristics in either of the extreme settings. To avoid unnecessary circuit complexity in this proof-of-concept demonstration, the circuit was confined to two switched states, recognizing that the filter could be readily generalized if need be to include additional in-between steps. The circuit could also be readily adapted for use with microelectromechanical switching devices, trading decreased bias-current requirements and even better linearity for decreased switching speed and a still exploratory state of technology. However, even with the use of conventional p-i-n diodes as switching elements, the circuit in its current configuration exhibits a notable third-order-intercept-point level of 46 dBm at passband frequencies, qualifying the filter for use in many front-end applications.

Acknowledgment

The filter circuit was assembled by Film Microelectronics Inc., Marlborough, MA, with the author expressing special thanks to J. W. Roman for his help in executing the project. The author is also very grateful to S. Kirchoefer, Naval Research Laboratory, Washington, DC, for his assistance with post-assembly issues.

References

[1] J. Uher and W. J. R. Hoefer, "Tunable microwave and millimeter-wave band-pass filters," *IEEE Trans. Microwave Theory Tech.*, vol. 39, pp. 643–653, Apr. 1991.

[2] Y.-H. Shu, J. A. Navarro, and K. Chang, "Electronically switchable and tunable coplanar waveguide-slotline band-pass filters," *IEEE Trans. Microwave Theory Tech.*, vol. 39, pp. 548–554, Mar. 1991.

[3] D. Peroulis, S. Pacheco, K. Sarabandi, and L. P. B. Katehi, "Tunable lumped components with applications to reconfigurable MEMS filters," in *IEEE MTT-S Int. Microwave Symp. Dig.*, vol. 1, 2001, pp. 341–344.

Christen Rauscher (S'73–M'75–SM'82–F'89) received the Diploma degree in electrical engineering and Doctorate degree from the Swiss Federal Institute of Technology, Zürich, Switzerland, in 1969 and 1975, respectively.

From 1976 to 1978, he studied the nonlinear behavior of GaAs FETs at Cornell University, Ithaca, NY, and at the Naval Research Laboratory (NRL), Washington, DC. He subsequently joined the NRL, where he is currently Staff Consultant to the Microwave Technology Branch, after having spent a sabbatical year at the Los Alamos National Laboratory, Los Alamos, NM, from 1985 to 1986, and having served from 1986 to 2002 as Head of the NRL's Solid-State Circuits Section. His current research interests are centered on the pursuit of new high-frequency filter concepts and the exploitation of nonlinear signal interaction in semiconductor devices at microwave, millimeter-wave, and optical frequencies.

Dr. Rauscher was an IEEE Distinguished Microwave Lecturer. He was the recipient of a 1976 International Fellowship presented by the Swiss National Science Foundation, the 1987 IEEE Microwave Prize, the 1991 NRL Sigma Xi Applied Science Award presented by the Scientific Research Society of America, the 1999 IEEE Microwave Application Award, and the 2002 Engineering Sciences Award presented by the Washington Academy of Sciences.